

Determination of kinetic parameters associated to pyrolysis or combustion processes

Alain BRILLARD & Jean-François BRILHAC

Lab. Gestion des Risques et Environnement, Université de Mulhouse, France

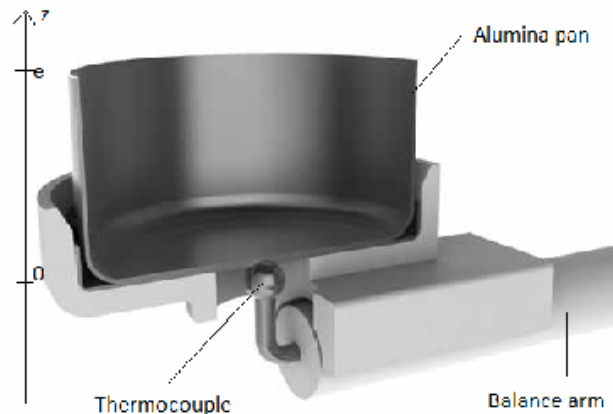
19 Octobre 2018 JANO'12 AL HOCEIMA

1 Objective

The purpose of this presentation is to describe and to analyze different models accounting for the thermal degradation of combustible materials (biomass, coals, waste, mixtures...), when submitted to a controlled temperature ramp and under non-oxidative or oxidative atmospheres. Because of the possible rarefaction of fossil fuels, the analysis of different combustible materials which could be used as (renewable) energy sources is important. In industrial conditions, the use of such materials in energy production is performed under very high temperature ramps (up to 10^5 °C/min in industrial pulverized boilers). But the analysis of the thermal degradation of these materials usually first starts under much lower temperature ramps (less than 100 °C/min and usually around 5 °C/min), to avoid diffusional limitations which modify the thermal degradation process.

2 Thermal degradation in a thermobalance

Very small amounts of such materials (few milligrams) are put in the metallic pan of a thermobalance (here Texas Instruments Q600).



A gas flow (pure nitrogen or mixture nitrogen and oxygen) is injected in the thermobalance.

The thermobalance is heated under a controlled low temperature ramp (few °C/min) to restrict possible diffusional limits inside the material.

The evolution of the temperature, from ambient temperature to 900 °C, is controlled with high accuracy. The thermobalance further measures the remaining mass of the sample with a high precision along the whole experiment. It computes the mass loss rate along the experiment.

The file produced by the thermobalance is further analyzed for the determination of the kinetic parameters.

It is important to notice that even if high temperatures are reached no flames really occur during such experiments, even under synthetic air. Only small inflammations may occur during very short times.

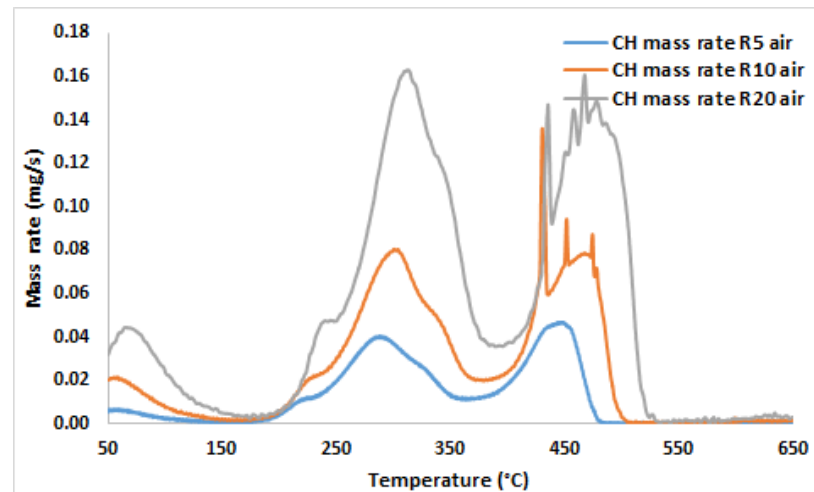


Figure 1: Small inflammations appearing on the second peak during the thermal degradation of coffee husks under air at different temperature ramps.

A first peak occurs in the temperature ramp 50-150 °C, which corresponds to the moisture evaporation stage. It will not be considered in the rest of the presentation as it is not the main purpose of an analysis of the pyrolysis or combustion processes.

All biomass are composed of three constituents: hemicellulose, cellulose and lignin, plus the carbon structure (in complement to ash, moisture...), which are known to degrade in different but superimposing temperature ranges. The mass loss rate curve presents peaks and shoulders, whose numbers depend on the material.

The relative fractions of these constituents depend on the material and the bonds between them influence the thermal degradation of the material. These relative fractions may be partly deduced observing the mass loss rate curve (relative importance of the shoulders or peaks).

The mass and mass rate curves for a Cameroonian wood residue exhibit two main peaks. On the left-hand side of the first peak appears a shoulder. Between the two peaks the mass rate curve does not fall to 0. The mass curve does not end at 0, because of the presence of ash.

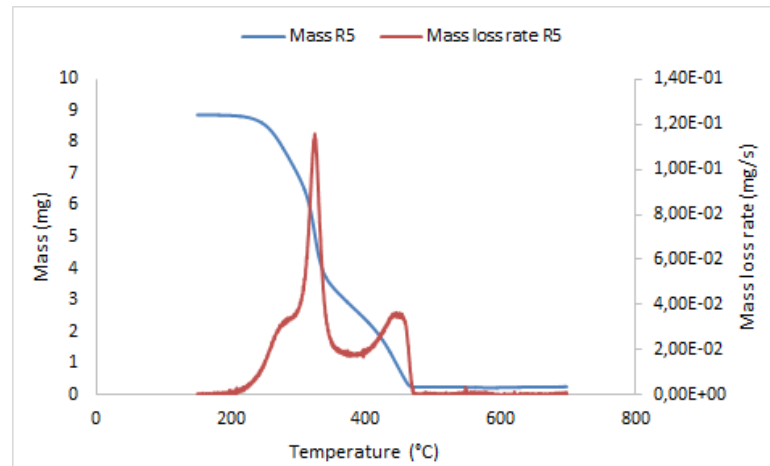


Figure 2: Mass and mass loss rate curves for a Cameroonian wood residue, temperature ramp of 5 °C/min, under synthetic air.

Based on these assumption and observation, different models have been proposed for a simulation of the thermal degradation in a thermobalance of a material considered either as global or as the sum of different constituents which are being degraded in an almost independent way, as their chains are intricate with the carbon structure.

These models only simulate the mass losses during the experiments to determine the kinetic parameters. They do not simulate the gaseous or particulate emissions.

More complex models are proposed which are based on balances: masses of the different chemical species which are emitted during the experiments, momentum, energy. These models intend to also simulate the gaseous and particulate emissions. But they involve much more parameters to be determined. Such complex models involve many equations and need a dedicated software for their numerical resolution.

In the different available models, constants have to be determined from the experimental results. They are called kinetic parameters and they are characteristics of the material and of the experimental conditions. The resolution of a

model has thus to be coupled with an optimization procedure which determines the optimal set of kinetic parameters.

The purpose of this conference is to present one of simplest models:

the Extended Independent Parallel Reaction = EIPR model

Finally more complicated models will be briefly introduced.

3 Kinetic modeling through the EIPR model

3.1 Description of the model

The pan is few millimeters long and high. Variations of the pyrolysis or combustion processes with respect to the space variables may thus be omitted and one can reasonably consider the evolution of the mass with respect to only the time parameter.

The EIPR model superimposes the thermal degradations of three or four constituents of the material (in the case of a biomass: the hemicellulose (H), cellulose (C) and lignin (L) constituents of the sample, plus its char under an oxidative atmosphere), whose masses are supposed to evolve in an almost

independent way. It leads to a unique set of kinetic parameters for each constituent of the sample. The initial mass m_{ini} of the sample is decomposed as $m_{ini} = m(0) + m_{ash} + m_{hum}$, where $m(0)$ (resp. m_{ash} , m_{hum}) is the mass of volatiles which will be emitted and of char which will be produced (resp. ashes, moisture) in the sample.

At time t , the remaining mass $m(t)$ of the sample which can produce volatiles and char is given by

$$m(t) = \sum_{i=H,C,L} m_i(t) = \sum_{i=H,C,L} \left(m_i(0) - m_{vol,i}^e(t) - m_{char,i}^p(t) \right), \quad (1)$$

where $m_i(t)$ is the mass of volatiles and of char contained in the constituent i ($i = H, C, L$) of the sample at time t , $m_i(0)$ is the initial mass of the

constituent i , which may be computed as a fraction of the overall mass of the sample: $m_i(0) = c_i m(0)$ (with $c_H + c_C + c_L = 1$), $m_{vol,i}^e(t)$ is the mass of volatiles emitted by the constituent i of the sample ($i = H, C, L$), at time t and $m_{char,i}^p(t)$ is the mass of char produced from the constituent i of the sample ($i = H, C, L$), at time t . These relative fractions c_i of hemicellulose, cellulose and lignin may be determined using a chemical protocol.

Under a non-oxidative atmosphere and assuming first-order reactions for each constituent, the mass of volatiles emitted from the constituent i ($i = H, C, L$) is supposed to evolve with respect to the time parameter according to

$$\frac{dm_{vol,i}^e}{dt}(t) = k_i(T(t)) (m_i(0) - m_{vol,i}^e(t)); m_{vol,i}^e(0) = 0, \quad (2)$$

where $k_i(T)$ obeys an Arrhenius law: $k_i(T) = A_i \exp(-Ea_i/RT)$.

Under an oxidative atmosphere, the material loses its volatiles and its char is also consumed. For each constituent, the mass of volatiles emitted is supposed to be proportional to the mass of char produced, that is

$$\frac{m_{vol,i}^e(t)}{m_{char,i}^p(t)} = \frac{\tau_{vol,i}}{\tau_{char,i}},$$

with $\tau_{vol,i} + \tau_{char,i} = 1$, $\tau_{vol,i}$ (resp. $\tau_{char,i}$) being the fraction of volatiles (resp. char) contained in the constituent i at time t . These coefficients $\tau_{vol,i}$ have to be estimated "by hand".

The mass of volatiles emitted from the constituent i ($i = H, C, L$) is here supposed to evolve with respect to the time parameter according to

$$\frac{dm_{vol,i}^e}{dt}(t) = k_i(T(t)) \left(m_i(0) - \frac{m_{vol,i}^e(t)}{\tau_{vol,i}} \right); m_{vol,i}^e(0) = 0. \quad (3)$$

Under an oxidative atmosphere, the mass of char remaining at time t in the constituent i of the sample at time t can be decomposed as $m_{char,i}(t) = m_{char,i}^p(t) - m_{char,i}^c(t)$, where $m_{char,i}^c(t)$ represents the mass of char consumed at time t among that ($m_{char,i}^p(t)$) which is produced from the constituent i of the sample ($i = H, C, L$).

The mass of char is supposed to evolve with respect to time t according to a first-order equation, as for the volatiles, but written as ($i = H, C, L$)

$$\begin{aligned}
 \frac{dm_{char,i}^c}{dt}(t) &= k_{comb}(T(t)) m_{char,i}(t) P_{O_2}, \\
 &= k_{comb}(T(t)) \left(m_{char,i}^p(t) - m_{char,i}^c(t) \right) P_{O_2}, \\
 &= k_{comb}(T(t)) \left(\frac{\tau_{char,i}}{\tau_{vol,i}} m_{vol,i}^e(t) - m_{char,i}^c(t) \right) P_{O_2},
 \end{aligned} \tag{4}$$

where P_{O_2} is the oxygen pressure which is constant during the experiment ($P_{O_2} = 2.026 \times 10^4$ Pa).

The kinetic constant $k_{comb}(T)$ also obeys an Arrhenius law:

$$k_{comb}(T) = A_{comb} \exp\left(-\frac{E_{a_{comb}}}{RT}\right).$$

Under an oxidative atmosphere, the coupled system of six ordinary differential equations has to be solved, with zero initial conditions

$$\left\{ \begin{array}{l} \frac{dm_{vol,i}^e}{dt}(t) = k_i(T(t)) \left(m_i(0) - \frac{1}{\tau_{vol,i}} m_{vol,i}^e(t) \right), \\ m_{vol,i}^e(0) = 0, \\ \frac{dm_{char,i}^c}{dt}(t) = k_{comb}(T(t)) \left(\frac{\tau_{char,i}}{\tau_{vol,i}} m_{vol,i}^e(t) - m_{char,i}^c(t) \right) P_{O_2}, \\ m_{char,i}^c(0) = 0. \end{array} \right. \quad (5)$$

The problems (2) or (5) are solved in the GRE lab using the Scilab numerical software (ode routine) with given initial guesses of the (6 or 8) kinetic parameters.

Notice that in the right-hand side of this coupled problem (5), only first-order (linear) functions with respect to the unknowns $m_{vol,i}^e(t)$ and $m_{char,i}^c(t)$ are used.

To determine the optimal values of the kinetic parameters, an error is built which has to be minimized (through Scilab datafit routine). For example:

$$error = \sum_{j=1} \left(\left(\frac{dm}{dt} \right)_{exp} (t_j) - \left(\frac{dm}{dt} \right)_{sim} (t_j) \right)^2,$$

where the simulated mass loss rate taken at time t_j is given under a non-oxidative atmosphere as $\left(\frac{dm}{dt} \right)_{sim} (t_j) = \sum_{i=H,C,L} \frac{dm_{vol,i}^e}{dt} (t_j)$ and under an oxidative atmosphere as

$$\frac{dm}{dt} (t) = \sum_{i=H,C,L} \left(\begin{aligned} &k_i (T (t)) \left(m_i (0) - \frac{1}{\tau_{vol,i}} m_{vol,i}^e (t) \right) \\ &+ k_{comb} (T (t)) \left(\frac{\tau_{char,i}}{\tau_{vol,i}} m_{vol,i}^e (t) - m_{char,i}^c (t) \right) P_{O_2} \end{aligned} \right).$$

3.2 Simulation of the thermal degradation of oil palm kernels under air with the EIPR model

Dérivée R10 air

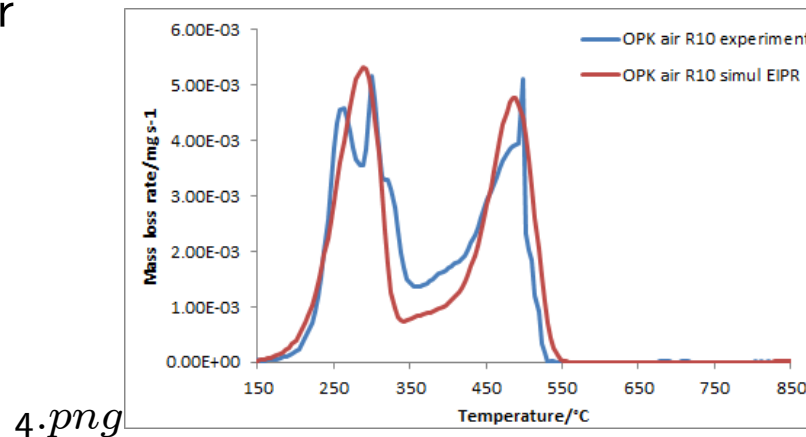


Figure 3: Simulation of the thermal degradation of oil palm kernels under air (temperature ramp 5 °C/min).

Four constituents (hemicellulose, cellulose, lignin and char) are here considered to be decomposed in an almost independent way.

For this material, the optimal values of the kinetic parameters (A in 1/s) and Ea in kJ/mol), of the fractions of the three constituents and of the volatile fractions are obtained through the EIPR model as:

A_H	4.0×10^6	A_L	8.7	c_H	0.29	$\tau_{vol,H}$	0.60
Ea_H	93000	Ea_L	54000	c_C	0.32	$\tau_{vol,C}$	0.65
A_C	1.1×10^{10}	A_{comb}	3.6×10^4	c_L	0.39	$\tau_{vol,L}$	0.50
Ea_C	143000	Ea_{comb}	160000				

and the maximal difference between the experimental and simulated mass loss rate curves is equal to 2.0×10^{-3} %/s, which has to be compared to the maximal mass loss rate curve, approximately 5.0×10^{-3} %/s.

3.3 Advantages of the EIPR model

The EIPR model returns values of the kinetic parameters which are global in time but for each constituent of the material, the number of such constituents depending on the material and on the experiments (pyrolysis or combustion).

The EIPR model allows simulating the thermal degradation of the material (mass and mass loss curves), with a quite satisfying accuracy.

The resolution of the ordinary differential equations associated to the EIPR model is easy and does not require any complex software.

The EIPR model is a quite performing method, but many unknowns to be determined in a system of 3 or 6 first-order differential equations, with superimposition of the thermal degradations of the constituents. Some of these

parameters (the c_i of the constituents of the lignocellulosic material) may be determined through further chemical experiments on the material).

The optimization procedure needs to be helped "by hand", which means that the values of the kinetic parameters have to be tested pair by pair, before using the datafit routine which optimizes the pre-selected values of the kinetic parameters. The reasons are:

- the intricate character of the degradations of the constituents,
- the high values of the kinetic parameters, which are linked to narrow and superimposing peaks.

Would a treatment of the problem as an inverse one help? A mathematical treatment of the problem should help: uniqueness of the kinetic parameters.

A kinetic compensation effect may occur between the pre-exponential factor and the activation energy.

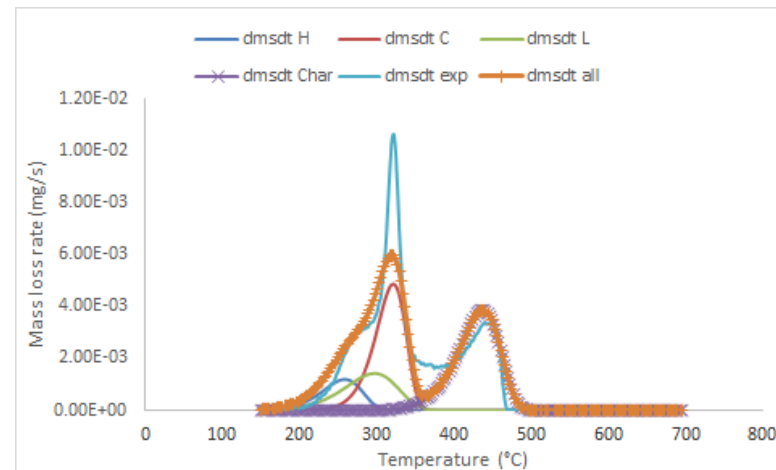


Figure 4: Superposition of the degradations of the four constituents of a Cameroonian woody biomass.

Clearly the degradations of the four constituents occur in superimposing temperature ranges.

3.4 Influence of the temperature ramp

The temperature ramp influences the thermal degradation of a material, as shifts appear on the mass loss rate curves when the temperature ramp increases.

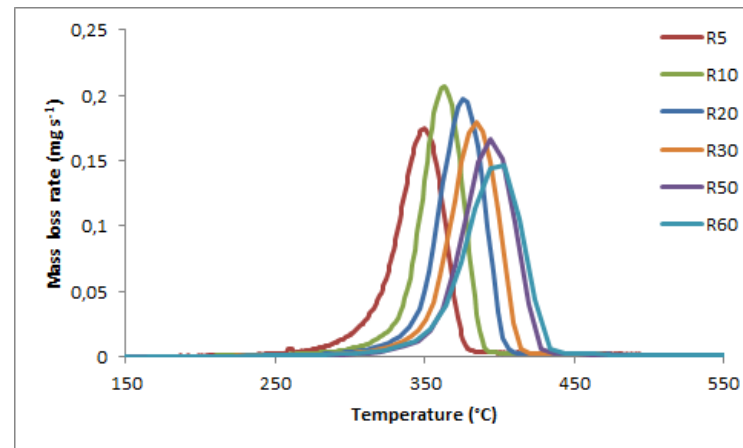


Figure 5: Influence of the temperature ramp on the thermal degradation of cotton residue under nitrogen.

The simulation of the thermal degradations of the same material under different temperature ramps but with the same kinetic parameters fails.

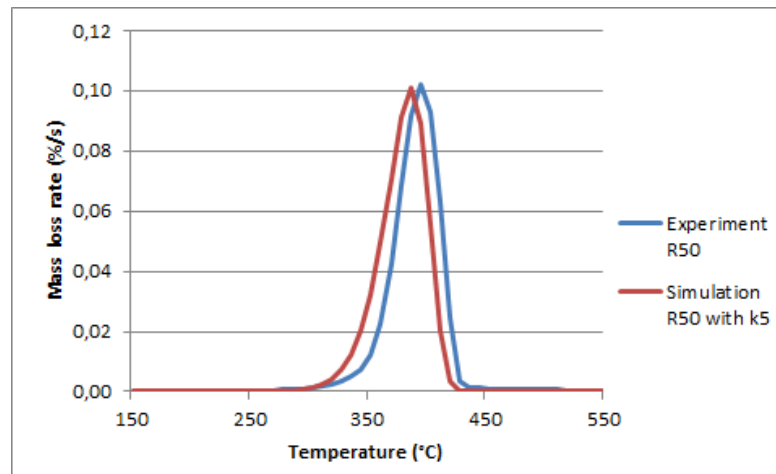


Figure 6: Simulation of the thermal degradation of cotton residue under temperature ramp of 50 °C/min with the kinetic parameters determined at a temperature ramp of 5 °C/min.

This may be the consequence of diffusional limitations which occur in the ma-

terial and which increase with the temperature ramp.

In [7], a heat transfer model has been proposed which brings corrections to the temperature really acting in the material. The temperature is supposed to evolve in the sample according to the classical heat transfer equation

$$\frac{\partial T}{\partial t}(z, t) - a \frac{\partial^2 T}{\partial z^2}(z, t) = 0, \text{ in } [0, e] \times [0, \infty], \quad (6)$$

where e is the thickness of the cotton sample and the thermal diffusibility coefficient a is given through $a = \frac{\lambda}{\rho c}$ with:

- λ thermal conductivity of cotton, approximately equal to 0.038 W/mK,

- ρ density of cotton, approximately equal to 40 kg/m^3 ,
- c specific heat coefficient of cotton, approximately equal to 1.725 kJ/kg .

Because of the structure of the TA Q600 thermobalance, the boundary condition

$$\frac{\partial T}{\partial z}(0, t) = -\frac{1}{\lambda} \left(h(T_g(t) - T(0, t)) + \varepsilon\sigma \left((T_g(t))^4 - (T(0, t))^4 \right) \right)$$

is considered at $z = 0$ (upper surface of the sample in contact with the surrounding heated atmosphere). In this boundary condition, h (resp. ε , σ) is taken equal to $5 \text{ W/m}^2\text{K}$ (resp. 0.9 , $5.67 \times 10^{-8} \text{ W/m}^2\text{K}^4$) and $T_g(t)$ means

the temperature of the heated gas surrounding the cotton sample. The temperature $T_g(t)$ is measured in the thermobalance by a thermocouple located just under the crucible. The boundary condition $\frac{\partial T}{\partial z} \left(\frac{e}{2}, t \right) = 0$ is imposed on the mid-thickness ($z = e/2$, with $e = 0.001$ m) surface of the sample, thus considering a symmetry of the sample layer with respect to its mid-thickness. The temperature T starts at $t = 0$ from the room temperature: $T(z, 0) = 20^\circ\text{C} = 293.15$ K.

The above heat transfer problem is solved through an implicit finite difference method with $dt = 8950/896 = 9.99$ s and $dz = (e/2)/100 = 5.0 \times 10^{-6}$ m, using the numerical software Scilab.

In the model (2), $T(t)$, which was initially taken as the measured gas temperature $T_g(t)$, is replaced by the computed mean value $(T(0, t) + T(e/2, t))/2$.

Here is an example of the simulation with and without correction of the temperature really acting in the material.

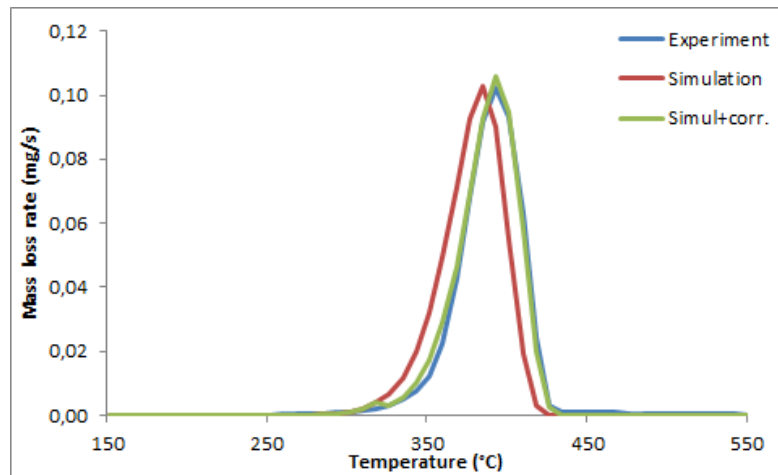


Figure 7: Comparison between the experimental mass loss rate curve (blue) under nitrogen and under temperature ramp equal to $50\text{ }^{\circ}\text{C}/\text{min}$, and the simulation with the values of the kinetic parameters obtained for a temperature ramp of $5\text{ }^{\circ}\text{C}/\text{min}$ without correction (red) or with the correction given by the mean value of the temperatures (green).

3.5 Choice of the reaction function

As already mentioned, first-order reaction functions have been used in the above simulations of the thermal degradations of materials. But other functions may be chosen. Here are some of them:

Avrami-Erofeev 2	$f(\alpha) = 2(1 - \alpha)(-\ln(1 - \alpha))^{1/2}$
Avrami-Erofeev 3	$f(\alpha) = 3(1 - \alpha)(-\ln(1 - \alpha))^{2/3}$
Avrami-Erofeev 4	$f(\alpha) = 4(1 - \alpha)(-\ln(1 - \alpha))^{3/4}$
Prout-Tompkins	$f(\alpha) = \alpha(1 - \alpha)$
Mampel 1 st order	$f(\alpha) = 1 - \alpha$
Mampel 2 nd order	$f(\alpha) = (1 - \alpha)^2$
Mampel 3 rd order	$f(\alpha) = (1 - \alpha)^3$

1-D diffusion	$f(\alpha) = 1/(2\alpha)$
2-D diffusion	$f(\alpha) = -1/\ln(1 - \alpha)$
3-D diffusion	$f(\alpha) = 1.5(1 - \alpha)^{2/3} / (1 - (1 - \alpha))^{1/3}$
Chain scission	$f(\alpha) = 2(\sqrt{\alpha} - \alpha)$

Some of them have a physicochemical interpretation. This may help for the choice. The change of a reaction function changes the values of the kinetic parameters. For example, for cotton residue under nitrogen

	$A \left(s^{-1} \right)$	$Ea \left(kJ \ mol^{-1} \right)$	$Error \left(mg \ s^{-1} \right)$
Mampel 1 ^{rst} order	3.7×10^{14}	201.3	9.1×10^{-4}
Avrami-Erofeev 2	3.5×10^{14}	205.3	1.6×10^{-2}
Prout-Tompkins	1.7×10^{14}	192.6	3.1×10^{-2}
Chain scission	7.7×10^{14}	201.0	2.6×10^{-2}

4 More complex models accounting for the thermal degradation of materials

As already indicated, the EIPR model only simulates the mass loss of the material along the pyrolysis or combustion processes.

More complex models have been proposed to also simulate the gaseous and particulate emissions which occur during such processes. For the construction of such models, the chemical species which are emitted during the thermal degradation process have to be determined first. In [10], the authors give a long list of possible chemical reactions which may occur during biomass pyrolysis, together with the corresponding kinetic parameters which are given Arrhenius expressions. Then the balance equations are written, see [11], in the case of 3 (main) chemical reactions and 5 gas species, which lead to a coupled system of $8+7$ equations (inside the particle and in a boundary layer around the particle).

4.1 Inside the spherical particle

- Conservation of each of the gaseous species ($k = 1, \dots, 5$)

$$\frac{\partial (\varepsilon \rho_{g,s} m_{k,s})}{\partial t} + \frac{1}{r^2} \frac{\partial}{\partial r} (r^2 N_{tg,s} M_{av} m_{k,s}) = \frac{D_{ke,s} \rho_{g,s}}{r^2} \frac{\partial}{\partial r} \left(r^2 \frac{\partial m_{k,s}}{\partial r} \right) + \sum_l \varepsilon R_l \gamma_{kl} M_k,$$

with $l = 3$.

- Total molar balance of gas mixture

$$\frac{\partial (\varepsilon c_{t,s})}{\partial t} + \frac{1}{r^2} \frac{\partial}{\partial r} (r^2 N_{tg,s}) = \sum_l \sum_k \varepsilon R_l \gamma_{kl}.$$

- Energy balance equation

$$\frac{\partial (C_{ps}\rho_s T_s)}{\partial t} + \frac{1}{r^2} \frac{\partial}{\partial r} \left(r^2 N_{tg,s} M_{av,s} C_{pg,s} T_s \right) = \frac{\lambda_e}{r^2} \frac{\partial}{\partial r} \left(r^2 \frac{\partial T_s}{\partial r} \right) + \sum_l \varepsilon R_l (-\Delta H_l).$$

- Carbon mass balance

$$\frac{\partial W_C}{\partial t} = - \left(2 \frac{\eta + 1}{\eta + 2} R_1 + R_2 \right) M_C.$$

4.2 In a gas boundary layer

- Conservation of each of the gaseous species ($k = 1, \dots, 5$)

$$\frac{\partial (\rho_g m_k)}{\partial t} + \frac{1}{r^2} \frac{\partial}{\partial r} (r^2 N_{tg} M_{av} m_k) = \frac{D_{ke} \rho_g}{r^2} \frac{\partial}{\partial r} \left(r^2 \frac{\partial m_k}{\partial r} \right) + R_3 \gamma_{k3} M_k.$$

- Total molar balance of gas mixture

$$\frac{\partial c_t}{\partial t} + \frac{1}{r^2} \frac{\partial}{\partial r} (r^2 N_{tg}) = \sum_k R_3 \gamma_{k3}.$$

- Energy balance equation

$$\frac{\partial (C_{pg} \rho_g T_g)}{\partial t} + \frac{1}{r^2} \frac{\partial}{\partial r} (r^2 N_{tg} M_{av} C_{pg} T_g) = \frac{\lambda_g}{r^2} \frac{\partial}{\partial r} \left(r^2 \frac{\partial T_g}{\partial r} \right) + R_3 (-\Delta H_3).$$

Initial and boundary conditions are added to this problem.

4.3 Other complex models

In [12], the authors introduce a simpler model, starting with the conservation law

$$\varepsilon \frac{\partial \rho_g}{\partial t} + \frac{1}{r^2} \frac{\partial}{\partial r} \left(r^2 \rho_g v_g \right) = S_{mass},$$

in the case of a spherical particle, where ε is the porosity of the particle (which may evolve along the combustion process), ρ_g is the gas density, v its velocity and S_{mass} represent the mass sources due to a transfer to the gas phase. The

balance of linear momentum is written using Darcy's law as

$$\varepsilon \frac{\partial \rho_g v_g}{\partial t} = -\frac{\partial p}{\partial r} - \frac{\mu}{k} - v_g - C \rho_g v_g |v_g|,$$

where p is the pressure, μ the viscosity, k the permeability and C is a constant. The convection+diffuse transport of the gaseous species inside the particle is written as

$$\frac{\partial \rho_{i,g}}{\partial t} + \frac{1}{r^2} \frac{\partial}{\partial r} \left(r^2 \rho_{i,g} v_g \right) = \frac{1}{r^2} \frac{\partial}{\partial r} \left(r^2 \frac{D_{i,eff}}{M_i} \frac{\partial \rho_{i,g}}{\partial r} \right) + \sum w_{k,i,gas},$$

where $w_{k,i,gas}$ is a reaction term. Finally the energy conservation is written as

$$\frac{\partial \sum_i \rho_i C_{p,i} T}{\partial t} = \frac{1}{r^2} \frac{\partial}{\partial r} \left(r^2 \lambda_{eff} \frac{\partial T}{\partial r} \right) + \sum w_k H_k.$$

Appropriate boundary and initial conditions are also added.

In [13], the authors introduce quite similar balance equations but in a steady regime.

Of course, for the resolution of such coupled and complex systems of evolution equations, numerical codes have to be built or dedicated software have to be used. In their paper [11], the authors indicate that they used Comsol multiphysics software for the resolution of this problem.

Such complex models have not been solved in the GRE lab. Interested readers are referred to the indicated references and to the further references these limited references contain.

As far as I know, existence and uniqueness results have never been proved for such coupled systems of evolution equations, although first they are based on balance equations and second they are certainly not "singular" systems. A theoretical numerical resolution of such systems should be developed.

5 Conclusion

Throughout this presentation, different methods and models accounting for the thermal degradation of combustible materials under controlled temperature ramps and non-oxidative or oxidative atmospheres have been presented. A focus on the EIPR model has been presented, as it is simple to solve. It gives quite satisfying simulations of the mass loss along the pyrolysis or combustion process. Each method or model is based on hypotheses and presents limits, although the obtained simulation of the thermal degradation process is roughly acceptable. Mathematical analyses of the models should be done in order to also improve these simulations. The references listed below will help the interested readers for deeper understandings of modeling representing these realistic and useful experiments.

References

- [1] S. Vyazovkin, AK. Burnham, JM. Criado, LA. Perez-Maqueda, C. Popescu and N. Sbirrazuoli, *ICTAC Kinetics Committee recommendations for performing kinetic computations on thermal analysis data*. *Therm. Acta* 520 (2011), pp. 1–19, <http://doi.org/10.1016/j.tca.2011.03.034>.
- [2] M. Valente, A. Brillard, C. Schönnenbeck and JF. Brilhac, *Investigation of grape marc combustion using thermogravimetric analysis. Kinetic modeling using an extended independent parallel reaction (EIPR)*. *Fuel Proces. Technol.* 131 (2015), pp. 297–303. <http://dx.doi.org/10.1016/j.fuproc.2014.10.034>.
- [3] A. Brillard, JF. Brilhac and M. Valente, *Modelization of the grape marc pyrolysis and combustion based on an extended independent parallel re-*

action and determination of the optimal kinetic constants. Comp. Appl. Math. 36(1) (2017), pp. 89-109. DOI 10.1007/s40314-015-0216-5.

- [4] JJM. Orfao, FJA. Antunes and JL. Figueiredo, *Pyrolysis kinetics of ligno-cellulosic materials - three independent reactions model. Fuel* 78 (1999), pp. 349-358. PII: S0016-2361(98)00156-2.

- [5] T. Damartzis, D. Vamvuka, S. Sfakiotakis and A. Zabaniotou, *Thermal degradation studies and kinetic modeling of cardoon (Cynara cardunculus) pyrolysis using thermogravimetric analysis (TGA). Bioresour Technol.* 102 (2011), pp. 6230–6238. doi:10.1016/j.biortech.2011.02.060.

- [6] J. Yu, N. Paterson, J. Blamey and M. Millan, *Cellulose, xylan and lignin interactions during pyrolysis of lignocellulosic biomass. Fuel* 191 (2017), pp. 140–149. doi:10.1016/j.fuel.2016.11.057.

- [7] A. Brillard, D. Habermacher and JF. Brilhac, *Thermal degradations of used cotton fabrics and of cellulose: kinetic and heat transfer modeling*, Cellulose, 24(3) (2017), pp. 1579-1595. DOI 10.1007/s10570-017-1200-6.
- [8] P. Gilot, A. Brillard, C. Schönnenbeck and JF. Brilhac, *A simplified model accounting for the combustion of pulverized coal char particles in a drop tube furnace*, Energy and Fuels (2017). DOI: 10.1021/acs.energyfuels.7b01756.
- [9] A. Brillard, JF. Brilhac and P. Gilot, *A second-order finite difference method for the resolution of a boundary value problem associated to a modified Poisson equation in spherical coordinates*. Appl. Math. Model. 49 (2017), pp. 182–198. <http://dx.doi.org/10.1016/j.apm.2017.04.034>.

- [10] A. Anca-Couce and R. Scharler, *Modelling heat of reaction in biomass pyrolysis with detailed reaction schemes*. Fuel 206 (2017), pp. 572–579. <http://dx.doi.org/10.1016/j.fuel.2017.06.011>.
- [11] AK. Sadhukhan, P. Gupta and RK. Saha, *Modeling and experimental studies on single particle coal devolatilization and residual char combustion in fluidized bed*. Fuel 90 (2011), pp. 2132-2141, doi:10.1016/j.fuel.2011.02.009.
- [12] B. Peters, A. Džiugys and R. Navakas, *A shrinking model for combustion/gasification of char based on transport and reaction time scales*. Mechanika 18(2) (2012), pp. 177-185.

- [13] K. Annamalai and IK. Puri, *Combustion science and engineering*. CRC Series in Computational Mechanics and Applied Analysis. CRC Press, Boca Raton, 2007.